Study of low-energy magnetic excitations in single-crystalline $CeIn_3$ by inelastic neutron scattering

2003 J. Phys.: Condens. Matter 15 3741

(http://iopscience.iop.org/0953-8984/15/22/308)

INSTITUTE OF PHYSICS PUBLISHING JOURNAL OF PHYSICS: CONDENSED MATTER

J. Phys.: Condens. Matter **15** (2003) 3741–3749 PII: S0953-8984(03)60928-8

Study of low-energy magnetic excitations in single-crystalline $CeIn_3$ by inelastic neutron scattering

W Knafo[1], S Raymond[1], B Fåk[2], G Lapertot[1], P C Canfield[1,3] and J Flouquet[1]

[1] CEA-Grenoble, DRFMC/SPSMS, 38054 Grenoble Cedex, France
[2] ISIS Facility, Rutherford Appleton Laboratory, Chilton, Didcot, Oxon OX11 0QX, UK
[3] Ames Laboratory, Iowa State University, Ames, IA 50011, USA

Received 6 March 2003
Published 23 May 2003
Online at stacks.iop.org/JPhysCM/15/3741

Abstract

Inelastic neutron scattering experiments were performed on single crystals of the heavy-fermion compound $CeIn_3$ for temperatures below and above the Néel temperature, T_N. In the antiferromagnetically ordered phase, well-defined spin-wave excitations with a bandwidth of 2 meV are observed. The spin waves coexist with quasielastic (QE) Kondo-type spin fluctuations and broadened crystal-field (CF) excitations below T_N. Above T_N, only the QE and CF excitations persist, with a weak temperature dependence.

1. Introduction

A quantum critical point (QCP) occurs in the heavy-fermion (HF) compound $CeIn_3$ under a hydrostatic pressure of $P_C = 25$ kbar. This corresponds to a transition at $T = 0$ K from a magnetically ordered to a disordered state. It was found that at least up to 23 kbar the ground state is antiferromagnetically ordered with a propagation vector $\boldsymbol{k} = (1/2, 1/2, 1/2)$. At ambient pressure the Néel temperature is $T_N = 10.1$ K and the staggered magnetization is $m_0 = 0.5\ \mu_B$ [1, 2]. $CeIn_3$ becomes superconducting below $T_C = 200$ mK in the vicinity of P_C [3, 4]. More generally, the appearance of unconventional superconductivity around P_C in HF systems is supposed to be related to the enhancement of magnetic fluctuations when $T_N \simeq 0$.

$CeIn_3$ crystallizes in the cubic $AuCu_3$ structure, and hence the magnetic fluctuations are expected to be three dimensional (3D). This is confirmed by resistivity measurements, which show a $\Delta\rho = T^{3/2}$ non-Fermi liquid (NFL) behaviour at the critical pressure, as expected for 3D fluctuations in spin-fluctuation theories [5, 6]. Recently, a new family of HF compounds was discovered [7], $Ce_mT_nIn_{3m+2n}$, which is composed of alternating layers of $CeIn_3$ and TIn_2 stacked along the c-direction with T = Ir, Rh or Co. Their main interest arises from the layered structure that is thought to induce two-dimensional (2D) fluctuations that would enhance the superconductivity more than 3D fluctuations near T_C [8]. Indeed, $CeCoIn_5$ has a

superconducting state at ambient pressure below $T_C = 2.3$ K, the highest T_C observed up to now in HF systems [9]. These recent results motivated us to reinvestigate the common building brick of these quasi 2D compounds: the 3D HF $CeIn_3$.

Previous inelastic neutron scattering (INS) studies on powder samples of $CeIn_3$ [10, 11] showed the existence of a crystal-field (CF) excitation at $\Delta_{CF} \simeq 12$ meV with a large broadening ascribed to the Kondo effect. In this work, we present new INS measurements on single crystals, which due to new flux growth methods are now sufficiently large for such studies. These measurements show the existence of well-defined spin-wave excitations in the magnetically ordered phase, which coexist with quasielastic (QE) Kondo-type spin fluctuations and the previously observed broadened CF excitations.

2. Experimental details

The single crystals used in this study were grown by the self-flux method [12]. A first set of neutron scattering measurements was carried out on the time-of-flight chopper spectrometer MARI at ISIS, using incident energies of 22 and 60.3 meV. The corresponding energy resolutions were approximately 2 and 5 meV respectively. Because of the strong neutron absorption cross-section of In, the single crystals were cut to a thickness of 2 mm and used in transmission geometry. A total of 30 crystals with total weight of 13 g were aligned and glued to a thin aluminium plate, which was mounted in a closed-cycle refrigerator. The mosaicity of the assembly was approximately 6°. Measurements were performed in the (hhl) plane, with an angle between the incident wavevector and the [001] direction of 2.5° and 30°.

A second set of neutron scattering measurements was made on the triple-axis spectrometer IN22 at the ILL (Grenoble, France). Pyrolytic graphite was used for the vertically focusing monochromator and the horizontally focusing analyser. A PG filter in the scattered beam was used to suppress higher-order contamination, and final neutron energies of 8.05 and 14.7 meV were used, giving energy resolutions of 0.5 and 1.0 meV respectively. Two thin plates of the assembly used on MARI were aligned on an aluminium support and mounted in a helium flow 'orange' cryostat. The total mass of the sample was about 1 g and the mosaicity 0.5°. The (hhl) scattering plane was investigated.

3. Results

3.1. Crystal-field excitation and quasielastic line

For the two crystals orientations used on MARI and at temperatures of $T = 5$, 15 and 150 K, we recorded $(\boldsymbol{Q}, E)$ intensity maps for $0 < Q < 10$ Å^{-1} and $E < 30$ meV, where $\boldsymbol{Q}$ is the wavevector transfer and E is the energy transfer. Despite strong phonon contamination from both the $CeIn_3$ sample and the Al support, we observed an excitation around 12 meV which was independent of the crystal orientation and whose intensity decreased with Q. The temperature dependence of the 12 meV excitation obtained for $Q < 2$ Å^{-1} is shown in figure 1. The excitation shows only a very slight softening and broadening as the temperature goes from the ordered state at $T = 5$ K to the paramagnetic state at $T = 15$ K. At much higher temperatures, $T = 150$ K, the excitation is partly suppressed. Figure 2 shows the wavevector dependence of the excitation spectrum at $T = 5$ K. The peak at 12 meV observed at low Q (integration over $0 < Q < 2$ Å^{-1}) disappears at higher wavevectors (integration over $7.5 < Q < 7.8$ Å^{-1}), reflecting its magnetic nature. The contribution around 20 meV, seen only at high Q, is due to phonons. The Q and T dependence of the 12 meV excitation, as illustrated in figures 1

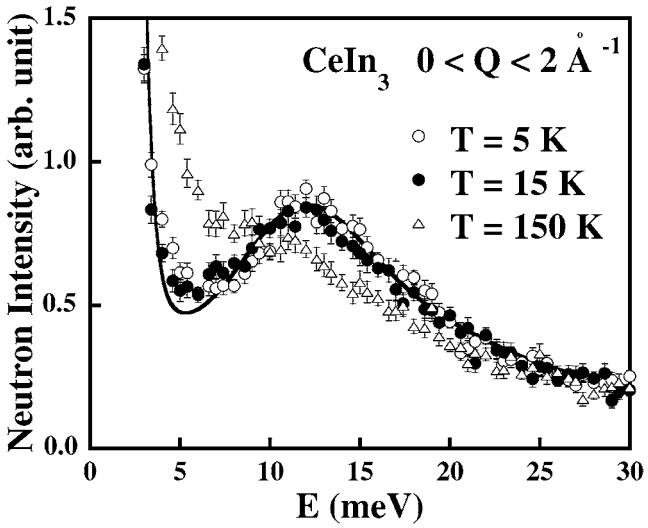

Figure 1. Energy scans at different temperatures obtained on the MARI spectrometer using an incident energy of 60.3 meV and integrating over Q values between 0 and 2 $Å^{-1}$. The solid curve shows the total fit for $T = 5$ K.

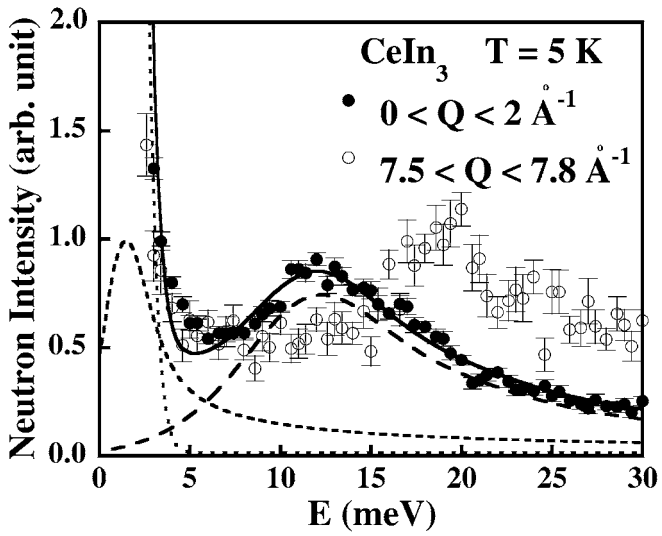

Figure 2. Energy scans at different wavevectors obtained on the MARI spectrometer using an incident energy of 60.3 meV at $T = 5$ K. The long dashed, short dashed and dotted curves show the CF, QE, and incoherent contributions of the small Q spectrum respectively, while the solid curve shows the total fit.

and 2, clearly show its magnetic origin; it corresponds to the CF excitation observed in powder samples by Lawrence and Shapiro [10] and Murani *et al* [11].

The cubic environment of Ce^{3+} in $CeIn_3$ can be treated in terms of Stevens operators by the following CF Hamiltonian: $H_{CF} = B_4(O_4^0 + 5O_4^4)$ [13]. This Hamiltonian splits the $J = 5/2$ spin–orbit level of Ce^{3+} into a Γ_8 quartet and a Γ_7 doublet. In the case of $CeIn_3$, susceptibility measurements indicate that $B_4 > 0$ [14], implying that the ground state is Γ_7. This has been

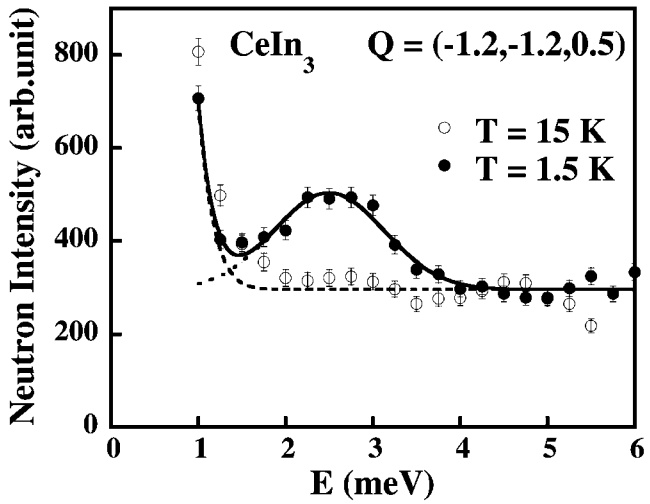

Figure 3. Energy scans at $\boldsymbol{Q} = (-1.2, -1.2, 0.5)$ for temperatures of $T = 1.5$ and 15 K obtained on the IN22 spectrometer using a final energy of 14.7 meV.

confirmed by polarized neutron scattering measurements, which also reveals an admixture of Γ_8 to the ground state Γ_7 in the ordered phase [15]. The excitation observed here at 12 meV then corresponds to the $\Gamma_7 \rightarrow \Gamma_8$ excitation.

In addition to the 12 meV CF excitation, it is clear from the data that there is an additional QE component to the scattering. The low-Q data at $T = 5$ K were therefore analysed using three components: an incoherent elastic peak, a QE spin-fluctuation contribution, and a CF excitation. Since the different contributions partly overlap, we fixed the width (half width at half maximum, HWHM) Γ_{QE} of the QE contribution to $k_B T_K = 0.86$ meV where $T_K = 10$ K is the Kondo temperature. The results of the analysis at $T = 5$ K give a CF splitting of $\Delta_{CF} = 10.6 \pm 0.2$ meV and a broadening of the CF levels (HWHM) of $\Gamma_{CF} = 5.7 \pm 0.2$ meV. No significant difference in the values of the CF excitations was found for the different orientations of the crystal. At $T = 15$ K, the resulting CF splitting is $\Delta_{CF} = 9.4 \pm 0.2$ meV and its width is $\Gamma_{CF} = 6.0 \pm 0.2$ meV. The observed slight softening of Δ_{CF} is related to the splitting of the CF levels below T_N.

3.2. Spin wave

The dispersive mode that appears below T_N was first observed using the MARI chopper spectrometer. Because of the 3D character of this mode, the study of its dispersion was continued using the IN22 triple-axis spectrometer. Energy scans up to 6 meV energy transfer were measured for different values of the wavevector transfer $\boldsymbol{Q}$. Figure 3 shows spectra of $CeIn_3$ at $\boldsymbol{Q} = (-1.2, -1.2, 0.5)$ for $T = 1.5$ and 15 K. This corresponds to the reduced wavevector $\boldsymbol{q} = \boldsymbol{Q} - \boldsymbol{\tau} - \boldsymbol{k} = (0.3, 0.3, 0)$, where $\boldsymbol{\tau} = (-1, -1, 1)$ is a reciprocal lattice vector and $\boldsymbol{k} = (-1/2, -1/2, -1/2)$ is a magnetic propagation vector (wavevectors are expressed in reciprocal lattice units (rlu) with 1 rlu $= 2\pi/a$, where $a = 4.689$ Å is the lattice parameter). Figure 3 clearly shows that the excitation present at $T < T_N$ disappears for $T > T_N$. For each wavevector $\boldsymbol{q}$, the excitation was fitted by a Gaussian whose width corresponds to the instrumental resolution. The strong dispersion of this excitation in the three main directions of the crystal is shown in figure 4. Since the direction of the ordered moment in $CeIn_3$ is unknown

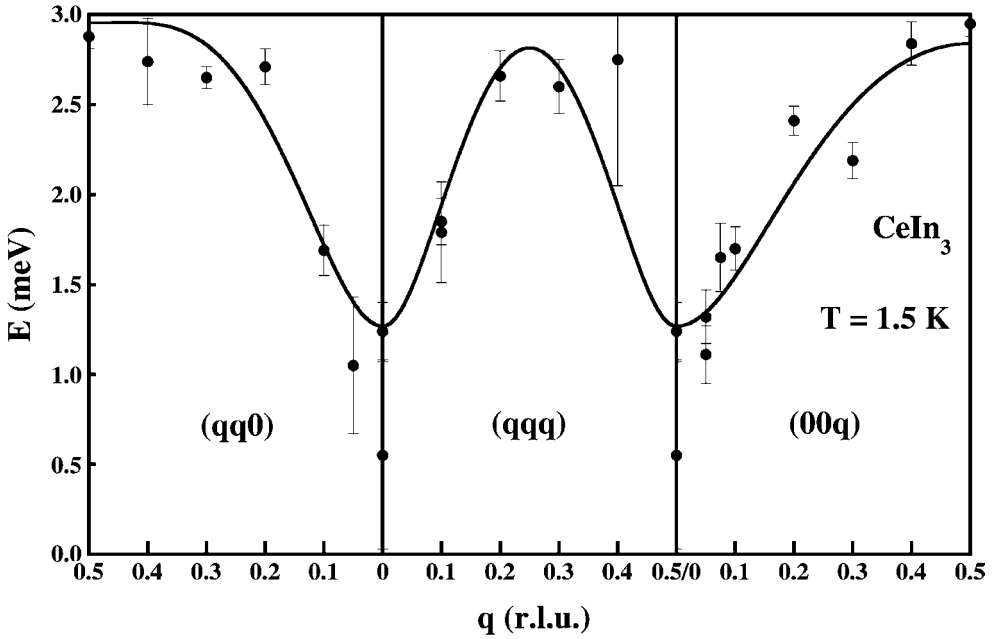

Figure 4. Spin-wave dispersion of $CeIn_3$ along the three main directions $(0, 0, q)$, $(q, q, 0)$ and (q, q, q) at $T = 1.5$ K, obtained on the IN22 spectrometer using a final energy of 14.7 meV. The solid curve is a fit obtained using the molecular-field random-phase approximation. rlu is reciprocal lattice unit(s) (see text).

and our sample is in a multidomain state, it is not possible to determine the polarization of the excitation; it will be assumed to be transverse as for a conventional spin wave.

Supposing that the CF energy is of the same order as the exchange interaction, it seems appropriate to treat the spin wave using the so-called molecular-field random-phase approximation [16]. Writing the exchange Hamiltonian as

$$H_{ex} = -\sum_{i,j} I_{ij} \boldsymbol{J}_i \boldsymbol{J}_j \tag{1}$$

gives the general dispersion relation

$$E(\boldsymbol{q}) = \{[\Delta - M^2 I(\boldsymbol{q})][\Delta - M^2 I(\boldsymbol{q}+\boldsymbol{k})]\}^{1/2}, \tag{2}$$

where $\boldsymbol{k}$ is the propagation vector of the ordered state, $I(\boldsymbol{q})$ the Fourier transform of the exchange interaction I_{ij}, and Δ the splitting of the Γ_7 doublet into $\Gamma_{7,1}$ and $\Gamma_{7,2}$ due to the molecular and anisotropy fields. The transition matrix element between the ground state $\Gamma_{7,1}$ and the first excited state $\Gamma_{7,2}$ is given by $M^2 = |\langle\Gamma_{7,2}|J^\alpha|\Gamma_{7,1}\rangle|^2 (\alpha = + \text{ or } -)$. Considering only the nearest neighbour exchange I_1 [along (1,0,0)] and the next nearest neighbour exchange I_2 [along (1,1,0)], the exchange interaction is

$$\begin{aligned} I(\boldsymbol{q}) = {} & 2I_1[\cos(2\pi q_x) + \cos(2\pi q_y) + \cos(2\pi q_z)] \\ & + 2I_2[\cos(2\pi(q_x - q_y)) + \cos(2\pi(q_y - q_z)) + \cos(2\pi(q_z - q_x)) \\ & + \cos(2\pi(q_x + q_y)) + \cos(2\pi(q_y + q_z)) + \cos(2\pi(q_z + q_x))]. \end{aligned} \tag{3}$$

In a two sub-lattice picture constituted of alternating (1,1,1) planes where the spins are up or down, I_1 would correspond to the antiferromagnetic exchange between spins from different sublattices and I_2 would correspond to the ferromagnetic exchange between spins from the

same sublattice. A global fit to the dispersion curves of equation (2) is shown in figure 4. It gives the exchange terms $M^2 I_1 = -0.354 \pm 0.040$ meV and $M^2 I_2 = 0.028 \pm 0.013$ meV and the Γ_7 splitting $\Delta = 2.812 \pm 0.480$ meV. The corresponding spin-wave gap is: $\delta = E(\mathbf{0}) = 1.28$ meV.

The exchange energy can be expressed by $E_{ex} = \frac{2J(J+1)}{3} I(\mathbf{0})$. Taking the wavefunctions of $\Gamma_{7,1}$ and $\Gamma_{7,2}$ when there is neither exchange nor distortion [17] gives us an approximated square transition matrix element $M^2 = 2.78$ thus $I(\mathbf{0}) = -0.64 \pm 0.18$ meV. With $J = 5/2$, we obtain $E_{ex} \simeq 3.71$ meV. The ratio $\Delta_{CF}/|E_{ex}| \simeq 3$ then permits us to conclude that the CF energy is of the same order as the exchange interaction that justifies the treatment of the spin wave using the molecular-field random-phase approximation.

4. Discussion

4.1. Kondo temperature

We have analysed the Q-independent excitations using two contributions, one corresponding to QE scattering and the other to a CF transition. Since these excitations overlap with each other and with the incoherent peak (see figure 2), the energy, width and weight of the different contributions extracted from the data depend on the model used for the fitting. This is illustrated by the scatter in the estimates of Δ_{CF}, Γ_{CF} and Γ_{QE} found in the literature [10, 11, 18, 19]. At low temperatures, the QE excitation corresponds to the spin fluctuations of the Γ_7 electronic level, which are attributed to the Kondo effect. Its width (HWHM) Γ_{QE} corresponds to the Kondo temperature. A Kondo temperature of $T_K = 10$ K at a pressure of $P = 19$ kbar was obtained in ^{115}In-NQR measurements by Kawasaki *et al* [20]. It is likely that below this pressure the anomaly at T_N in the $1/T_1$ temperature variation masks the T_K anomaly. We assume therefore that T_K has a very slight variation for pressures below $P = 19$ kbar, so that it is only slightly smaller than 10 K at ambient pressure. Resistivity measurements give a Kondo scattering maximum at $T_M \simeq 50$ K [4], which corresponds to the high Kondo temperature $T_K^h = \sqrt[3]{T_K(\Delta_{CF}/k_B)^2}$ [21]. INS gives $\Delta_{CF} = 10.6$ meV which with $T_K^h = 50$ K leads to $T_K \simeq 8$ K. It is then reasonable to approximate the Kondo temperature by $T_K \simeq 10$ K in $CeIn_3$ at ambient pressure. For the INS measurement carried out at $T = 5$ K $< T_K$, we choose consequently to fix the QE width to $\Gamma_{QE} = k_B T_K = 0.86$ meV. The fact that $\Gamma_{CF} = 5.7$ meV is relatively large compared with $\Gamma_{QE} = 0.86$ meV is due to the larger spin fluctuations associated with the Γ_8 first excited level. In fact, the CF transition $\Gamma_7 \rightarrow \Gamma_8$ has a width corresponding to the convolution of the Γ_7 and Γ_8 widths $\Gamma_{QE}^{\Gamma_7} = \Gamma_{QE}$ and $\Gamma_{QE}^{\Gamma_8}$. We can approximate $\Gamma_{CF} \simeq \Gamma_{QE}^{\Gamma_7} + \Gamma_{QE}^{\Gamma_8}$ and thus estimate that $\Gamma_{QE}^{\Gamma_8} \simeq \Gamma_{CF} - \Gamma_{QE} = 4.84$ meV, which is effectively five times larger than Γ_{QE}.

4.2. Anisotropy

Even if the CF level is broad, it seems that the propagating spin waves can be described by considering Γ_7 as an 'isolated' doublet split by the anisotropy and exchange fields. Since this doublet originates from a six-fold degenerate $J = 5/2$ level, an anisotropy gap is expected in the spin-wave spectrum. We recall that in the isotropic case the spin-wave dispersion has no gap, since only the exchange is responsible for the splitting Δ.

The gap δ of the spin-wave excitation corresponds to its minimum energy that is obtained at $\boldsymbol{q} = (0, 0, 0)$. Since this excitation overlaps with the incoherent elastic scattering that reflects the experimental resolution and with the QE contribution of the spin fluctuations, the gap was not correctly obtained in the present neutron experiment. The given value of δ

Table 1. Characteristic physical quantities of $CeIn_3$ and $CePd_2Si_2$. Data are taken from [3, 4, 22, 24–28].

	$CeIn_3$	$CePd_2Si_2$
T_N (K)	10.1	10
$\boldsymbol{k}$	(1/2, 1/2, 1/2)	(1/2, 1/2, 0)
m_0 (μ_B)	0.50	0.62
δ (meV)	0.69	0.83
Band width (meV)	$\sim$2	$\sim$2
θ_P (K)	-50	-47[a]
T_K (K)	10	10
Δ_{CF} (K)	123	220 and 280
P_C (kbar)	26.5	28.6
T_C (mK)	200	430
γ[b] (mJ mol^{-1} K^{-2})	130	250

[a] DC susceptibility measurement along the a-axis.
[b] $\gamma = C/T$ at low T.

corresponds to the best fit to the data using the spin-wave model described above. An attempt to directly observe the gap using a smaller incident energy (and hence better resolution) on the cold triple-axis spectrometer IN12 (ILL) failed because of the strong indium absorption cross-section. A determination of the energy gap was also made by low-temperature specific heat measurements which exhibited a spin-wave contribution that leads to a gap $\delta = 0.69$ meV [22]. This suggests that the gap energy of 1.28 meV deduced from our INS measurements is somewhat overestimated.

The result of our spin-wave analysis is in good agreement with calculations made by Wang and Cooper [17] for Ce^{3+} ions under cubic CF and effective exchange field. They consider a molecular field along the c-axis, which can be approximated by $g\mu_B H_m = k_B T_N$, and calculate the level splitting as a function of $g\mu_B H_m/B_4$. Knowing that for $CeIn_3$ $T_N = 10.1$ K, $\Delta_{CF} = 10.6$ meV and hence $B_4 = 2.94 \times 10^{-2}$ meV ($\Delta_{CF} = 360B_4$), we have $g\mu_B H_m = 8.71 \times 10^{-1}$ meV $\simeq 30B_4$. For this value of $g\mu_B H_m/B_4$, Wang and Cooper calculate a Γ_7 splitting of about $40B_4 \simeq 1.2$ meV. Although we suppose that in our case the molecular field is not along the c-axis (see below), we believe that Wang and Cooper's calculations give the right order of the splitting Δ.

There are several indications that the moments are not along the c-axis. If the CF alone imposes the easy magnetization axis, the positive sign of B_4 in the CF Hamiltonian implies that the moments are along the [1,1,1] direction in the ordered phase. This is also supported by nuclear quadrupolar resonance measurements [23]. Although it is difficult to determine the moment direction of a cubic compound by neutron diffraction, some recent measurements also suggest that the moments are not along the c-axis [22].

4.3. Comparison with $CePd_2Si_2$

$CeIn_3$ seems to have a behaviour very similar to the HF compound $CePd_2Si_2$ which is antiferromagnetically ordered at ambient pressure and has the same kind of excitation spectrum with coexisting QE, CF and spin-wave excitations [24]. The characteristic energies are very close and, moreover, unconventional superconductivity appears at a similar external pressure [3]. A summary of the characteristic physical quantities of those two compounds is given in table 1. A comparison of the few differences between those two compounds can be made as follows. Firstly $CePd_2Si_2$ is tetragonal while $CeIn_3$ is cubic. Some characteristics such as

the CF splitting or the susceptibility anisotropy can be directly linked to anisotropy effects that result from those lattice structures. Then, the characteristic quantities T_C and γ are twice as large in $CePd_2Si_2$ as in $CeIn_3$, which could translate to an enhancement of the spin fluctuations in the tetragonal $CePd_2Si_2$. As a supplement to the studies of quasi 2D $Ce_mT_nIn_{3m+2n}$ compounds where T_C can reach more than 2 K, an alternative way to study the influence of anisotropy in strongly correlated systems could consequently be a detailed comparison between cubic $CeIn_3$ and tetragonal $CePd_2Si_2$.

5. Conclusion

We have performed the first INS measurements on single crystals of $CeIn_3$. The combined use of time-of-flight and triple-axis spectrometers allowed us to study both local and dispersive low-energy excitations. We found the coexistence below T_N of a spin wave with a QE component and a CF excitation. The CF levels are substantially broadened by Kondo-type spin fluctuations, which indicates the proximity to an intermediate valence state where the CF collapse. Despite the smearing of the CF levels, the observation of spin waves means that the ground state level in $CeIn_3$ is also relatively well defined. The challenge is then to understand how these excitations evolve on going toward a QCP where the hierarchy between the Kondo effect and the RKKY coupling is reversed while the CF should be close to a collapse.

Acknowledgments

We acknowledge the help of K Mony with sample preparation and x-ray characterization. We thank also A P Murani for many useful and stimulating discussions.

References

[1] Morin P, Vettier C, Flouquet J, Konczykowsky M, Lassailly Y, Mignot J M and Welp U 1988 *J. Low Temp. Phys.* **70** 377
[2] Benoit B, Boucherle J X, Convert P, Flouquet J, Palleau J and Schweizer J 1980 *Solid State Commun.* **34** 293
[3] Mathur N D, Grosche F M, Julian S R, Walker I R, Freye D M, Haselwimmer R K W and Lonzarich G G 1998 *Nature* **394** 39
[4] Knebel G, Braithwaite D, Canfield P C, Lapertot G and Flouquet J 2001 *Phys. Rev.* B **65** 24425
[5] Millis A 1993 *Phys. Rev.* B **48** 7183
[6] Moriya T and Takimoto T 1995 *J. Phys. Soc. Japan* **64** 960
[7] Thompson J D, Movshovich R, Fisk Z, Bouquet F, Curro N J, Fisher R A, Hammel P C, Hegger H, Hundley M F, Jaime M, Pagliuso P G, Petrovic C, Phillips N E and Sarrao J L 2001 *J. Magn. Magn. Mater.* **226–230** 5
[8] Monthoux P and Lonzarich G G 2001 *Phys. Rev.* B **63** 054529
[9] Petrovic C, Pagliuso P G, Hundley M F, Movshovich R, Sarrao J L, Thompson J D, Fisk Z and Monthoux P 2001 *J. Phys.: Condens. Matter* **13** L337
[10] Lawrence J M and Shapiro S M 1980 *Phys. Rev.* B **22** 4379
[11] Murani A P, Taylor A D, Osborn R and Bowden Z A 1993 *Phys. Rev.* B **48** 10606
[12] Canfield P C and Fisk Z 1992 *Phil. Mag.* B **65** 1117
[13] Lea K R, Leask M J M and Wolf W P 1962 *J. Phys. Chem. Solids* **23** 1381
[14] Buschow K H J, De Wijn H W and Van Diepen A M 1969 *J. Chem. Phys.* **50** 137
[15] Boucherle J X, Flouquet J, Lassailly Y, Palleau J and Schweizer J 1983 *J. Magn. Magn. Mater.* **31–34** 409
[16] Buyers W J L, Holden T M and Perreault A 1975 *Phys. Rev.* B **11** 266
[17] Wang Y L and Cooper B R 1970 *Phys. Rev.* B **2** 2607
[18] Groß W, Knorr K, Murani A P and Buschow K H J 1980 *Z. Phys.* B **37** 123
[19] Lassailly Y, Burke S K and Flouquet J 1985 *J. Phys. C: Solid State Phys.* **18** 5737
[20] Kawasaki S, Mito T, Zheng G-Q, Thessieu C, Kawasaki Y, Ishida K, Kitaoka Y, Muramatsu T, Kobayashi T C, Aoki D, Araki S, Haga Y, Settai R and Ōnuki Y 2001 *Phys. Rev.* B **65** 020504

[21] Hanzawa K, Yamada K and Yosida K 1985 *J. Magn. Magn. Mater.* **47/48** 357
[22] Knafo W *et al* 2003 unpublished
[23] Kohori Y, Kohara T, Yamato Y, Tomka G and Riedi P C 2000 *Physica* B **281/282** 12
[24] Van Dijk N H, Fåk B, Charvolin T, Lejay P and Mignot J M 2000 *Phys. Rev.* B **61** 8922
[25] Grier B H, Lawrence J M, Murgai V and Parks R D 1984 *Phys. Rev.* B **29** 2664
[26] Demuer A, Jaccard D, Sheikin I, Raymond S, Salce B, Thomasson J, Braithwate D and Flouquet J 2001 *J. Phys.: Condens. Matter* **13** 9335
[27] Steeman R A, Mason T E, Lin H, Buyers W J L, Menovsky A A, Collins M F, Frikkee E, Nieuwenhuys G J and Mydosh J A 1990 *J. Appl. Phys.* **67** 5203
[28] Grosche F M, Julian F R, Mathur N D and Lonzarich G G 1996 *Physica* B **223/224** 50